Desalination and Water Treatment
www.deswater.com

doi: 10.1080/19443994.2015.1041049

57 (2016) 6116–6123
March

Taylor & Francis
Taylor & Francis Group

Kinetic and thermodynamic study of cobalt adsorption by spent coffee

Djillali Imessaoudene[a,*], Salah Hanini[b], Abdelkader Bouzidi[a], Abderrahmane Ararem[a]

[a]*Department of Chemistry, Centre de Recherche Nucléaire de Birine, BP 180, Ain oussera W. Djelfa, CP 17200, Algerie, Tel. +213 773971566; email: idjillali@yahoo.fr (D. Imessaoudene), Tel. +213 559492089; email: Bouzidiaek@yahoo.fr (A. Bouzidi), Tel. +213 551208446; email: arareme@mail.com (A. Ararem)*

[b]*Department of Biomaterials and Transport Phenomena, Université Yahia Fares de Médéa, CP 26000, Algerie, Tel. +21325985200; email: s_hanini2002@yahoo.fr*

Received 15 February 2014; Accepted 24 March 2015

ABSTRACT

The biosorption of cobalt from aqueous solution onto a spent coffee (SC) was carried out to assess the effectiveness of the adsorbent used in the removal of Co(II) from aqueous solution by batch tests. Adsorption of Co(II) as a function of contact time, pH, and temperature was investigated. The kinetic study revealed that adsorption followed better a second-order type reaction with high correlation coefficient ($R^2 = 0.999$). Adsorption data were described using Freundlich and Langmuir models. The thermodynamic study for the Co(II) adsorption onto SC showed that the process was spontaneous with a raised affinity for Co(II) ($\Delta G^\circ < 0$ and $\Delta S^\circ > 0$), exothermic ($\Delta H^\circ < 0$), and occurred with physical adsorption mechanism ($E_a = 10.922$ kJ mol^{-1}).

Keywords: Cobalt; Adsorption; Kinetics; Thermodynamics

---

1. Introduction

The development of industrial activities using either radioactive or stable materials led to the release of a number of pollutants in the environment. Co(II) is a very toxic element affecting the environment and human health. Cobalt is used in many important industrial applications (for example, in metallurgy, dyes, and electronics industries), it is also a relatively abundant product in the nuclear reactors and it constitutes a source of radioactive waste from these installations [1]. Moreover, the presence of cobalt-60 in the environment resulting from these operations was a question of concern because of its radiotoxicity, its long half-life (10 years), and its high solubility in water. Therefore, it remains a radionuclide which can penetrate durably in the biogeochemical cycle of the living organisms.

As a conventional method for pollutant removal, adsorption has been developed as an efficient and economical method for the removal of trace metals from wastewaters and water supplies [2]. That is why a variety of adsorbents, including clays, zeolites, agricultural waste biomass [3], *Mentha arvensis* [1], agro-wastes [4], and mushroom [5].

Numerous techniques have been developed for the removal of heavy metals ions from the contaminated sites. Phytoremediation is a growing field of research

---

*Corresponding author.

Presented at the 3rd Annual International Conference on Water (CI.EAU 2013), 18–20 November 2013, Algiers, Algeria

in environmental studies. The major advantages of phytoremediation over conventional treatments include cost-effectiveness and environmental-friendliness [5]. Biosorption is one of the possible innovative techniques involved in the remediation of heavy metals and radionuclides from wastewaters and the subsurface environment. Compared with conventional treatment methods, biosorption is seen as a low-cost, energy-saving alternative, which has high efficiency and selectivity for absorbing metals in low concentrations and operates over broad ranges of pH and temperature [4].

Selection of an appropriate adsorbent is often based on price, raw material availability, and its easy use [6]. The spent coffee (SC) can play a key role in wastewater treatment processes; it would be useful in decontamination of wastewater and allows an alternative usage of unused waste. Columns tests can also be investigated using this kind of materials because of their rigidity and permeability [7].

In the present study, a SC was used as a biosorbent to explore its potential for the removal and recovery of cobalt from aqueous solutions.

2. Materials and methods

All chemicals were of analytical grade (HCl, NaOH, and $Co(NO_3)_2.6H_2O$). Solutions were prepared by dissolving a known quantity in deionized water (North Star ULTRA system: resistivity 1 MΩ cm).

The SC used in this study was coming from cafeterias and washed with deionized water to remove dust and other materials. The washed materials were then completely dried at ambient air for 1 d and then at 80˚C during 24 h, crushed using a crusher (RETSCH, type RM100), and sieved to 200–400 µm with strainer (RETSCH AS200 Digit). Finally, the obtained material was stored in desiccators until use. The principal characteristics of the prepared biosorbent are given in Table 1.

Sorption experiments were carried out in batch method where 0.1 g of SC was contacted with 50 mL of Co^{2+} solution (10 mg L^{-1}) in 100 mL-Erlenmeyer flasks, preequilibrated at temperature 20˚C, and initial pH was 5.8 (adjusted by HCl or NaOH). The flasks were sealed with para-film to avoid evaporation then shaken for required time at 250 rpm. After that, suspensions were filtrated through a 0.45 µm cellulose nitrate filter (Sartorius). The residual concentration of Co^{2+} was measured using an A-Analyst 400 atomic absorption spectrometer from PerkinElmer Inc.

Table 1
Principal characteristics of SC

Ash content (%)	0.712
Water holding capacity (%)	262.35
Humidity (%)	5.88
Swelling ratio (%)	133.33
Apparent density (g/cm^3)	0.52
Real density (g/cm^3)	2.154
PZC	5.65

Adsorption capacity (q_e) at equilibrium (mg g^{-1}) and the uptake percentage of Co^{2+} were determined using the following equations:

$$q_e = \frac{(C_0 - C_e) \times v}{m} \quad (1)$$

$$\text{uptake } (\%) = \frac{C_0 - C_e}{C_0} \times 100 \quad (2)$$

where m is the mass of adsorbent (g), V is the volume of the solution (L), C_0 is the initial concentration of metal (mg L^{-1}), and C_e is the equilibrium metal concentration (mg L^{-1}).

3. Results and discussion

3.1. Characterization

FTIR spectra obtained before and after biosorption are very similar (Fig. 1). The broad adsorption peak at around 3,473 cm^{-1} originating from the presence of carboxylic acid and amino groups were supported by the emergence of the peaks at 1,088, 1,641, and 1,543 cm^{-1} allocated to –OH, C=O, and amine groups, respectively [7,8]. The peaks 2,925 and 2,854 cm^{-1}

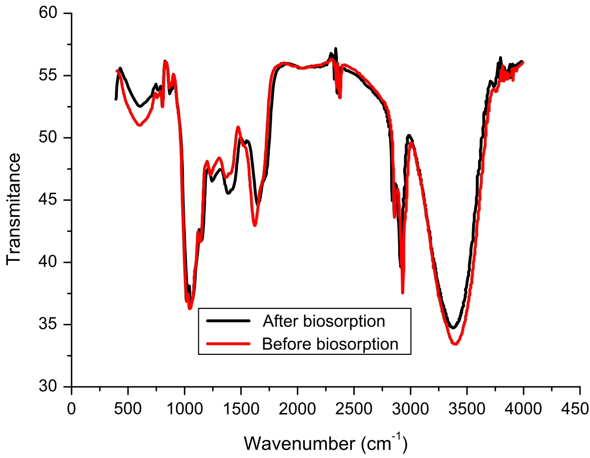

Fig. 1. FTIR spectra of SC before and after biosorption 199 mm × 139 mm (300 × 300 DPI).

could be allotted to the vibration of aliphatic groups CH. The peaks at 1,741 and 1,641 cm^{-1} could be ascribed to the C=O stretching in the carboxylic acids, anhydrides, and lactones. The bands at 1,462 and 1,246 cm^{-1} are assigned to the symmetric bending of CH$_3$. The peak located at 1,165 cm^{-1} is characteristic of the C–O–C vibration. The infrared bands are slightly shifted from the bands 3,473, 1,641, 1,543, 1,377, 1,088, and 613 cm^{-1} to 3,465, 1,635, 1,520, 1,379, 1,068, and to 609, respectively, demonstrating that the groups –OH, C=O, and the amino groups played a role in the Co^{2+} biosorption [7,9].

3.2. Effect of contact time

The effect of contact time was examined in the range of 0–120 min. Fig. 2 showed a fast biosorption process with three disparate phases. The higher rate of the first period advises that the biosorption was physical in nature and limited by the available sites on the biosorbent; easily accessible by the Co^{2+} [10,11]. At the second period, the rate was slowed down because the Co^{2+} ions met a higher resistance to penetrate deeper in the remaining intraparticulate active sites [12]. And so the plateau obtained by the extension of the reaction to 120 min did not lead to an improvement in the uptake percentage corresponding to the equilibrium state. The weak desorption is associated with the dispersion of Co^{2+} part, which did not reach inaccessible adsorbent surfaces and/or repulsed by the adsorbed ions, in aqueous solution [13].

3.3. Effect of solution initial pH

The pH is one of the most important parameter affecting adsorption process in aqueous solutions. Because the speciation of metals in solution depends on the pH, and at the same time the surface charge changes with the variation of the solution pH [14]. In order to determine the optimal pH value, the evolution of biosorption yield was examined over a range from 3.1 to 7.3.

The results presented on Fig. 3 showed that the uptake percentage of adsorbed Co^{2+} increased with the increase in the pH value up to 4, and then remained practically constant until pH 6.6, and then a second jump of the yield started. At lower pH, the solution concentrates in H$^+$ ions which will enter in competition with cobalt cations and will occupy most of the available biosorbent surface. Moreover the functional groups undergo a strong protonation, which confers on the biosorbent a positive total charge from which a repulsion force was established with the cobalt ions having a same charge [15,16]. The increase in the pH makes that the solution concentrated with free hydroxyls anions supporting the deprotonation of the biosorbent particles and increases by the fact that cobalt fixed by a phenomenon of electrostatic attraction [17,18]. Moreover, these OH$^-$ ions could play the role of bonds between the surface functions as positively charged and cobalt. Also, the surface charge can be supported by the value of PZC of SC (5.65). The surface charge of SC is positive at pH < 5.65, is neutral at pH 5.65, and is negative at pH > 5.65. At pH, greater than 5.65, SC becomes negatively charged [19].

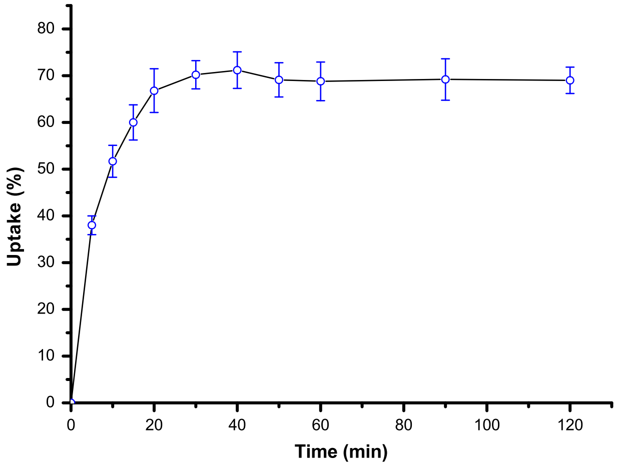

Fig. 2. Effect of contact time 202 mm × 141 mm (300 × 300 DPI).

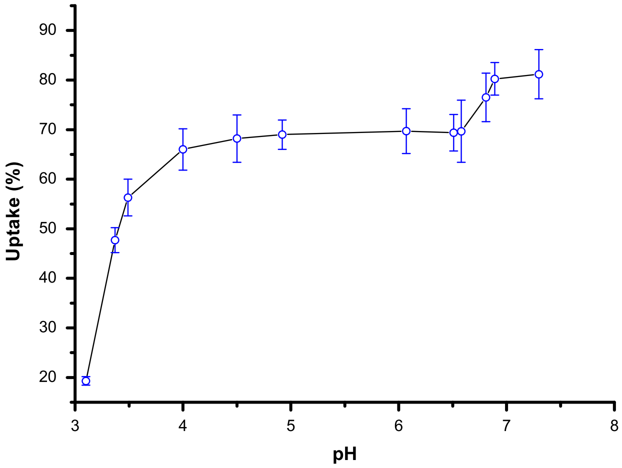

Fig. 3. Effect of solution initial pH 202 mm × 141 mm (300 × 300 DPI).

After, the yield jump at pH > 6.6 is probably due to the beginning of precipitation of the Co^{2+} ions [3].

3.4. Effect of temperature

To understand the temperature effect on the cobalt biosorption, experiments were also conducted at 10, 20, 30, 40, and 50°C. The uptake percentages at equilibrium are given in Fig. 4. Biosorption of Co^{2+} ions onto SC biomass were not considerably affected by temperature. Maximum yield (71.88%) was obtained with 10°C. Increase 10°C in temperature causes an average reduction in uptake percentage of 2.2%. This behavior may signify that adsorption occurred with electrostatic interactions, where the weakest bond can be broken with the increase in the temperature [1]. This indicates that the process was exothermic and of physical nature.

3.5. Kinetics modeling

The modeling of the kinetics experimental data allows a description of the uptake mechanisms and phenomena which control the biosorption process. In this work, three kinetic models were used to describe the Co^{2+} biosorption: the linearized forms of the pseudo-first-order, the pseudo-second-order, and the diffusion in liquid film given by Eqs. (3)–(5), respectively.

$$\ln (q_e - q_t) = \ln (q_e) - k_1 t \tag{3}$$

$$\frac{t}{q_t} = \frac{1}{k_2 q_e^2} + \frac{t}{q_e} \tag{4}$$

$$\ln (1 - (q_t/q_e)) = k_{fd} t \tag{5}$$

where q_t is the quantity of Co^{2+} adsorbed at time t (mg g^{-1}). k_1, k_2, and k_{fd} are the equations constants of the pseudo-first-order (mn^{-1}), the pseudo-second-order (g mg^{-1} min^{-1}), and the diffusion in liquid film, respectively.

The initial rate of uptake (H) was calculated as follows:

$$H = k_2 q_e^2 \tag{6}$$

The application of the pseudo-first-order kinetic model (Fig. 5) gave a satisfactory correlation coefficient ($R^2 = 0.992$); experimental and calculated q_e values were 3.459 and 3.741 mg g^{-1}, respectively.

The adsorption followed the second-order model (Fig. 6) with a correlation coefficient ($R^2 = 0.999$) and q_e value of 3.623 mg g^{-1}.

In fact, many of authors indicated that the kinetics of metals adsorption on different biosorbents is in conformity with the assumptions of the model of the pseudo-second-order [7]. The initial rate ($H = 1.761$ mg g^{-1} min^{-1}) indicated that the cobalt biosorption occurred promptly. According to Fig. 7, it is clear that the diffusion model in film is also valid for the cobalt retention where the correlation coefficient is $R^2 = 0.922$. This indicates that the mass transfer through film constitutes a limiting factor confirming

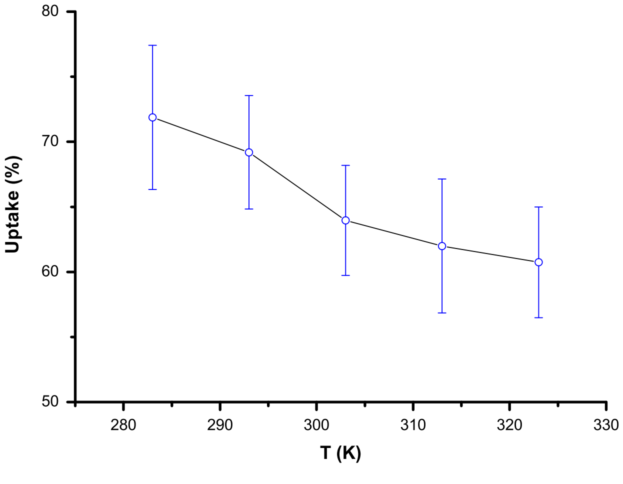

Fig. 4. Effect of temperature 202 mm × 141 mm (300 × 300 DPI).

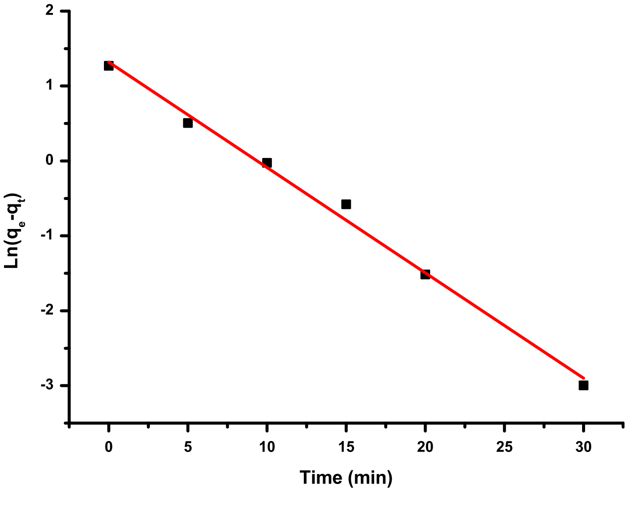

Fig. 5. pseudo-first-order kinetic model plot of Co^{2+} biosorption onto SC 209 mm × 148 mm (300 × 300 DPI).

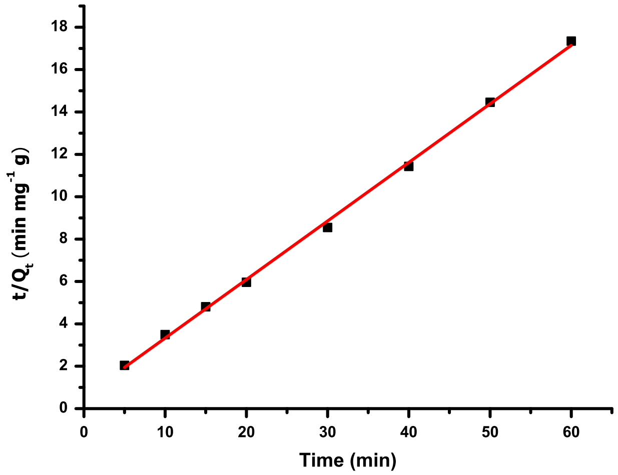

Fig. 6. Pseudo-second-order kinetic model plot of Co^{2+} biosorption onto SC 203 mm × 147 mm (300 × 300 DPI).

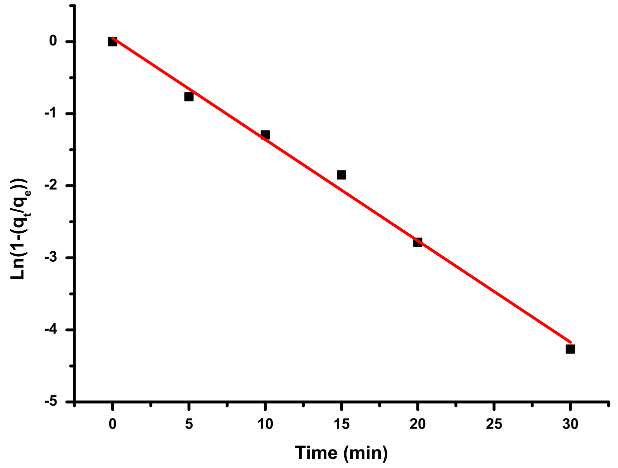

Fig. 7. Diffusion in liquid film model plot of Co2 + biosorption onto SC 210 mm × 148 mm (300 × 300 DPI).

the lower activation energy as shown (see activation energy section). Obtained results are presented in Table 2.

3.6. Thermodynamic study

The goal of this study is to explain or predict macroscopic phenomena and to calculate the thermodynamic parameters of this system. Thus, while being helped by the isotherms modeling adsorption, the calculation of these parameters is made possible by Eqs. (7) and (8).

$$\ln K_d = \frac{\Delta S^\circ}{R} - \frac{\Delta H^\circ}{RT} \quad (7)$$

$$\Delta G^\circ = \Delta H^\circ - T\Delta S^\circ \quad (8)$$

$$K_d = k_2 q_e^2 \quad (9)$$

where K_d is the distribution coefficient, ΔH° is the standard enthalpy (kJ mol^{-1}), ΔS° is the standard entropy (J mol^{-1} K^{-1}), R is the gas constant, T the temperature (K), and ΔG° is the standard Gibbs free energy (kJ mol^{-1}) (see Fig. 8).

The enthalpy and entropy values were obtained from the slope and intercepts of linear regression of ln K_d vs. $1/T$ and the standard Gibbs free energy values ΔG° were calculated from Eq. (8).

The negative values of ΔG° and ΔH° (Table 3) indicate that the Co^{2+} biosorption reaction was spontaneous and exothermic. Moreover the reaction was favored in spite of the fact that exothermic process supported by the decrease of ΔG° proportionally at the temperature. $\Delta S^\circ > 0$ showed the increase in the disorder at the solid–solution interface. Also, the negative changes of the free energy and the enthalpy together with positive change of the entropy indicated that the

Table 2
Kinetic parameters for Co^{2+} biosorption on SC

Model	Parameters	q_e (mg g^{-1})	Experimental
Pseudo-first-order	K_1 (min^{-1})	0.141	3.459
	q_e (mg g^{-1})	3.741	
	R^2	0.992	
Pseudo-second-order	K_2 (g mg^{-1} min^{-1})	0.134	
	q_e (mg g^{-1})	3.623	
	H (g mg^{-1} min^{-1})	1.761	
	R^2	0.999	
Diffusion in liquid film	K_{df}	0.141	
	R^2	0.922	

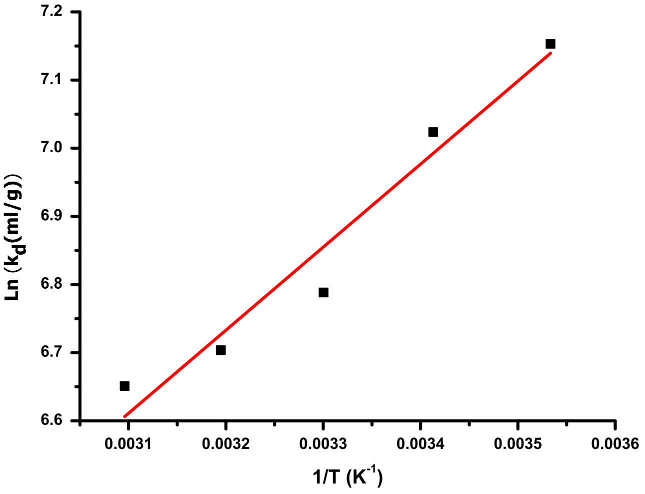

Fig. 8. Variation of the ln (K_d) according to the reverse of the temperature 203 mm × 147 mm (300 × 300 DPI).

biosorption reaction of cobalt on SC occurred with a raised affinity [7,20].

3.7. Activation energy

The activation energy of sorption was evaluated using the values of the pseudo-second-order rate constants k_2 at different temperatures (Fig. 9) by the Arrhenius equation (Eq. (10)).

$$\ln\frac{k_2(T_2)}{k_2(T_1)} = -\frac{E_a}{R}\left(\frac{1}{T_2} - \frac{1}{T_1}\right) \tag{10}$$

where R is the perfect gas constant (8.314 J mol^{-1} K^{-1}) and T is the temperature (K). The activation energy can be conceived as the minimum kinetic energy required for a given reaction to occur. The E_a value obtained (10.922 kJ mol^{-1}) is much below the energies corresponding to chemisorptions barriers (usually > 18 kJ mol^{-1}), suggesting that physical adsorption is operating where the attractive forces are of Van der Waals-type in addition to weak electrostatic forces, these assumptions made us to assume that the process is governed by the diffusion through the film layer around the particle [9].

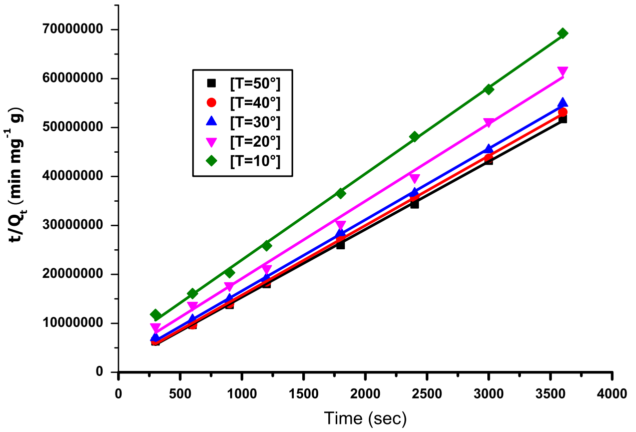

Fig. 9. Model of pseudo-second-order at different temperatures 210 mm × 148 mm (300 × 300 DPI).

3.8. Isotherm modeling

Isotherm studies were conducted at pH 6 using different initial concentrations of Co(II) with a fixed amount of SC. Freundlich and Langmuir isotherm models have been used to describe the equilibrium characteristics of adsorption. These isotherms are represented in the following equations:

$$q = K_F C^{1/n} \tag{11}$$

$$q = \frac{q_m K_L C}{1 + K_L C} \tag{12}$$

where q is the amount of solute adsorbed per unit weight of solid (mg g^{-1}), q_m is the maximum adsorption capacity of adsorbent per unit weight (mg g^{-1}), K_F and $1/n$ are Freundlich constants related to capacity and intensity of adsorption, respectively. K_L is the

Table 3
Thermodynamic parameters for the biosorption of cobalt onto SC

T (K)	K_d (mL g^{-1})	ΔG° (kJ mol^{-1})	ΔH° (kJ mol^{-1})	ΔS° (kJ mol^{-1} K^{-1})	R^2
283	1278.094	−16.822	−10.129	0.024	0.941
293	1122.850	−17.101			
303	887.347	−17.072			
313	815.443	−17.437			
323	773.561	−17.852			

Langmuir constant related to maximum monolayer adsorption capacity (see Fig. 10).

Adsorption isotherms for the adsorption of Co(II) onto SC are shown in Fig. 11. All constants obtained from nonlinear fit of the adsorption data to these isotherms are presented in Table 4 together with the correlation coefficients and normalized standard deviation (SD) which allow us to compare the validity of the isotherm equations more definitely.

$$\mathrm{SD}(\%) = 100 \times \sqrt{\frac{\sum\left[\left(\mathrm{q}_\mathrm{e}^{\exp} - q_\mathrm{e}^{\mathrm{cal}}\right)/q_\mathrm{e}^{\exp}\right]^2}{N-1}} \tag{13}$$

where superscripts "exp" and "cal" are the experimental and calculated values with the fitted parameters and N is the number of measurements.

The Freundlich isotherm parameter ($1/n$) that measures the adsorption intensity of Co^{2+} ions was less than unity (0.131). This implies that a significant adsorption may occur even at high Co^{2+} ion concentrations. The deviation of ($1/n$) from unity indicates a nonlinear adsorption that takes place on the heterogeneous surfaces. This behavior implies that the adsorption energy barrier increases exponentially as the fraction of filled sites on adsorbent increases [21]. K_F value provides quantitative information on the relative adsorption affinity towards the adsorbed cobalt cations.

Langmuir isotherm model was chosen to estimate the maximum adsorption capacity corresponding to complete monolayer coverage on the adsorbent. The cobalt adsorption capacity on SC at 293 K was 5.37 mg g^{-1}. This rate of adsorption capacity was compared in Table 5 with other adsorbents reported in the literature [22–24].

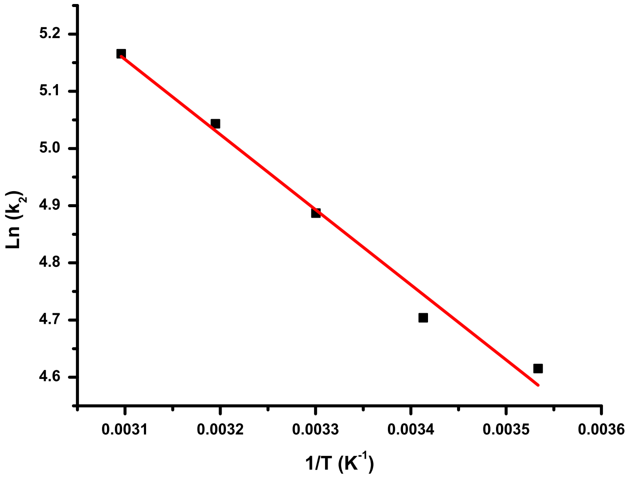

Fig. 10. Ln (k_2) against reciprocal temperature 203 mm × 147 mm (300 × 300 DPI).

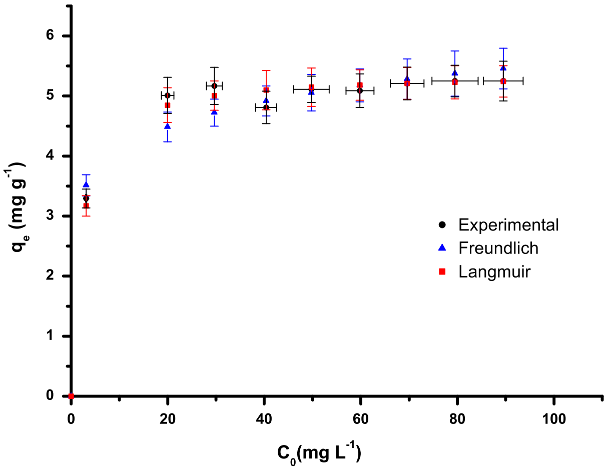

Fig. 11. Adsorption isotherms 202 mm × 141 mm (300 × 300 DPI).

Table 4
Isotherm models parameters for the adsorption of Co(II) onto SC

Isotherm	Parameters	Magnitude
Freundlich	$1/n$	0.131
	K_F ((mg$^{(1-1/n)}$) L$^{1/n}$ g^{-1})	3.03
	R^2	0.884
	SD (%)	1.86
Langmuir	$q_{\max}$ (mg/g^{-1})	5.37
	K_L (L/mg^{-1})	0.465
	R^2	0.998
	SD (%)	0.716

Table 5
Biosorption of Co(II) by different biosorbents

Adsorbent	q_m (mg g^{-1})	References
Foam (*Rhytidiadelphus*)	7.38	[2]
Chitosan	2.98	[22]
Arca shell	11.53	[23]
Green algae (spirulina)	0.01	[24]
SC	5.37	This study

4. Conclusion

The aim of this study was to synthesize a low-cost, nontoxic, and effective biosorbent constituted by SC and evaluate its adsorptive properties towards cobalt cations. The adsorption capacity of SC was found to be 5.37 mg g^{-1}.

Obtained results for Co^{2+} adsorption revealed that SC can be used as alternative adsorbent for removal of Co^{2+} in wastewater and also be suitable for the removal of other pollutants. The texture and rigidity of this material would allow us to test their feasibility in dynamic mode and therefore be able to handle large quantities of radioactive and/or stable liquid wastes.

Acknowledgments

This work is supported by the Nuclear Research Center of Birine in Algeria. The authors gratefully acknowledge the help rendered by all people who contributed to the realization of this work.

References

[1] H.N. Bhatti, A. Saleem, M.A. Hanif, Utilization of *Mentha arvensis* waste biomass for the removal of Pb (II) and Co(II) from aqueous solutions, Desalin. Water Treat. 51 (2013) 3335–3343.

[2] J. Marešová, M. Pipíška, M. Rozložník, M. Horník, L. Remenárová, J. Augustín, Cobalt and strontium sorption by moss biosorbent: Modeling of single and binary metal systems, Desalination 266 (2011) 134–141.

[3] H.N. Bhatti, R. Khadim, M.A. Hanif, Biosorption of Pb (II) and Co(II) on red rose waste biomass, Iran. J. Chem. Chem. Eng. 30 (2011) 81–87.

[4] A. Kausara, H.N. Bhatti, G. MacKinnon, Equilibrium, kinetic and thermodynamic studies on the removal of U(VI) by low cost agricultural waste, Colloids Surf. B 111 (2013) 124–133.

[5] H.N. Bhatti, M. Amin, Removal of zirconium(IV) from aqueous solution by *Coriolus versicolor*: Equilibrium and thermodynamic study, Ecol. Eng. 51 (2013) 178–180.

[6] N. AL-Ghezawi, M.A. Al-Anber Z.A. Al-Anber, T. El- Hasan, I. Al-Momani, Decontamination and adsorption modelling ofaqueous Pb^{2+} and Co^{2+} ions using natural inorganic materials: Tripoli (NT) and bentonite (NB), Desalin. Water Treat. 24 (2010) 336–343.

[7] D. Imessaoudene, S. Hanini, A. Bouzidi, Biosorption of strontium from aqueous solutions onto spent coffee grounds, J. Radioanal. Nucl. Chem. 298 (2013) 893–902.

[8] F. Çolak, N. Atar, A. Olgun, Biosorption of acidic dyes from aqueous solution by *Paenibacillus macerans*: Kinetic, thermodynamic and equilibrium studies, Chem. Eng. 150 (2009) 122–130.

[9] H. Eroglu, S. Yapici, C. Nuhoglu, E. Varoglu, An environmentally friendly process: Adsorption of radionuclide Tl-201 on fibrous waste tea, J. Hazard. Mater. 163 (2009) 607–617.

[10] M.V.B. Krishna, S.V. Rao, J. Arunachalam, M.S. Murali, S. Kumar, V.K. Manchanda, Removal of 137Cs and 90Sr from actual low level radioactive waste solutions using moss as a phytosorbent, Sep. Purif. Technol. 38 (2004) 149–161.

[11] F. Seliman Ayman, Affinity and removal of radionuclides mixture from low-level liquid waste by synthetic ferrierites, J. Radioanal. Nucl. Chem. 292 (2012) 729–738.

[12] D. Lu, Q. Cao, X. Cao, F. Luo, Removal of Pb(II) using the modified lawny grass: Mechanism, kinetics, equilibrium and thermodynamic studies, J. Hazard. Mater. 166 (2009) 239–247.

[13] A. Hanafi, Adsorption of cesium, thallium, strontium and cobalt radionuclides using activated carbon, J. At. Mol. Sci. 1 (2010) 292–300.

[14] H. Parab, M. Sudersanan, Engineering a lingo cellulosic biosorbent—Coir pith for removal of cesium from aqueous solutions: Equilibrium and kinetic studies, Water Res. 44 (2010) 854–860.

[15] P. Chakravarty, C.D. Dinesh, S.S. Neelotpal, P.S. Hari, Removal of copper (II) from wastewater by heartwood powder of *Areca catechu*: Kinetic and equilibrium studies, Desalin. Water Treat. 40 (2012) 194–203.

[16] A.E. Okoronkwo, S.J. Olusegun, Biosorption of nickel using unmodified and modified lignin extracted from agricultural waste, Desalin. Water Treat. 51 (2013) 1989–1997.

[17] H. Yazid, L. Amour, A. Terkmani, R. Maachi, Biosorption of lead from aqueous solution by biologically activated date pedicels: Batch and column study, Desalin. Water Treat. 51 (2013) 1690–1699.

[18] N. Balkaya, N. Bektas, Chromium (VI) sorption from dilute aqueous solutions using wool, Desalin. Water Treat. 3 (2009) 43–49.

[19] E.K. Guechi, F. Bendebane, A. Aisset, R. Malaoui, Sorption of mercury (II) from aqueous solution by Okoume sawdust, Desalin. Water Treat. 38 (2012) 285–292.

[20] W.H. Van Riemsdijk, G.H. Bolt, L.K. Koopal, J. Blaakmeer, Electrolyte adsorption on heterogeneous surfaces, J. Colloid Interface Sci. 109 (1986) 219–228.

[21] A. Ararem, O. Bouras, F. Arbaoui, Adsorption of caesium from aqueous solution on binary mixture of iron pillared layered montmorillonite and goethite, Chem. Eng. 172 (2011) 230–236.

[22] Y. Chen, J. Wang, The characteristics and mechanism of Co(II) removal from aqueous solution by a novel xanthate-modified magnetic chitosan, Nucl. Eng. Des. 242 (2012) 452–457.

[23] S. Dahiya, R.M. Tripathi, A.G. Hegde, Biosorption of heavy metals and radionuclide from aqueous solutions by pre-treated arca shell biomass, J. Hazard. Mater. 150 (2008) 376–386.

[24] K. Chojnacka, A. Chojnacki, H. Górecka, Trace metal removal by *Spirulina* sp. from copper smelter and refinery effluent, Hydrometallurgy 73 (2004) 147–153.